© 2014. Published by The Company of Biologists Ltd | Journal of Cell Science (2014) 127, 5157–5163 doi:10.1242/jcs.155911

SHORT REPORT

Nuclear actin and myocardin-related transcription factors control disuse muscle atrophy through regulation of Srf activity

Laura Collard[1,2,3], Gaëlle Herledan[1,2,3], Alessandra Pincini[1,2,3], Aline Guerci[1,2,3], Voahangy Randrianarison-Huetz[1,2,3] and Athanassia Sotiropoulos[1,2,3,*]

ABSTRACT

Skeletal muscle atrophy is a debilitating process that is associated with a wide variety of conditions including inactivity, disease and aging. Here, we demonstrate that the actin, myocardin-related transcription factors and serum response factor (actin–Mrtf–Srf) pathway is specifically downregulated in the muscle atrophy that is induced through disuse in mice. We show *in vivo* that the abolition of mechanical signals leads to the rapid accumulation of G-actin in myonuclei and the export of the Srf coactivator Mrtf-A, resulting in a decrease of Mrtf–Srf-dependent transcription that contributes to atrophy. We demonstrate that inhibition of the actin–Mrtf–Srf axis through overexpression of nuclear non-polymerizable actin, through pharmacological inhibition of Mrtf–Srf and through muscle-specific *Srf* deletion worsens denervation-induced atrophy. Conversely, maintenance of high levels of activity of Srf or Mrtfs in denervated muscle, through overexpression of constitutively active derivatives, counteracts atrophy. Altogether, our data provide new mechanistic insights into the control of muscle mass upon disuse atrophy by the actin–Mrtf–Srf pathway, highlighting Srf as a key mediator of mechanotransduction in muscle.

KEY WORDS: Actin, Atrophy, Skeletal muscle, Transcription

INTRODUCTION

Skeletal muscle wasting represents a major health problem because it is the consequence of a wide variety of pathological conditions, including inactivity (bed rest or nerve injury), starvation, chronic diseases and neuromuscular disorders.

Muscle atrophy always entails loss of organelles and cytoplasm, and involves protein-breakdown pathways (Bonaldo and Sandri, 2013). In particular, the ubiquitin-proteasome system induces the degradation of sarcomeric proteins, such as α-actin, through the muscle E3 ubiquitin ligase MuRF1 (Polge et al., 2011). In addition, disuse atrophy is associated with a decrease in the expression of genes encoding contractile proteins (Giger et al., 2009). This suggests that the control of muscle mass also stems from transcriptional and pre-translational regulatory processes. To date, it is unknown whether specific signaling pathways are involved in disuse muscle atrophy.

Serum response factor (Srf) is a member of the MADS-box transcription factor family. One major class of Srf targets is muscle-specific and comprises several genes encoding sarcomeric proteins (α-actins, myosins) (Pipes et al., 2006). The ability of Srf to regulate downstream target genes depends on its association with coactivators – including Ets-domain proteins, which are activated by MAPK, and myocardin-related transcription factors (Mrtfs), the nuclear accumulation of which is controlled by Rho GTPases and actin dynamics (Posern and Treisman, 2006). Using a mouse model of adult myofiber *Srf* deletion, we have previously reported that Srf is crucial for adult skeletal muscle hypertrophy, whereas it is not needed for myofiber maintenance (Guerci et al., 2012).

Here, we investigate the role of the actin–Mrtf–Srf pathway in skeletal muscle atrophy of different origins. We show that Srf activity is specifically downregulated by the abolition of mechanical cues and is governed by a rapid G-actin accumulation in myonuclei, which results in a decrease in intranuclear Mrtfs. Moreover, we demonstrate *in vivo* that denervation-induced muscle atrophy is aggravated by inhibiting the actin–Mrtf–Srf pathway and is counteracted by maintaining a high level of activity of either Srf or Mrtfs. Altogether, our results reveal the actin–Mrtf–Srf axis as a key pathway controlling disuse atrophy because its alteration directly impacts the extent of atrophy.

RESULTS AND DISCUSSION

Srf activity decreases upon disuse atrophy

To examine the contribution of Srf to skeletal muscle atrophy, we electroporated a Srf luciferase reporter construct into the tibialis anterior muscle of control mice, which showed a significant decrease in Srf transcription activity following denervation (Fig. 1A). As a consequence, the expression of Srf target genes, such as α-skeletal actin (*Acta1*) and *Srf*, which is its own target, was reduced in denervated gastrocnemius and plantaris, and tibialis anterior muscles (Fig. 1B; supplementary material Fig. S1A). Tallying with the diminished expression of *Srf* transcripts, a decreased Srf protein content was detected (Fig. 1C; supplementary material Fig. S1B). We then examined Srf subcellular localization within myofibers, as its extranuclear localization has been reported in atrophied rat muscles after 14 days of an 'intensive care unit model' (Ochala et al., 2011) and in beating-arrested neonatal rat cardiomyocytes (Lange et al., 2005); Srf extranuclear localization has also been associated with nuclear accumulation of MuRF2. However, up to 7 days post denervation, Srf protein was located inside myonuclei (supplementary material Fig. S1C), suggesting that, in this system and at this timing, the observed decrease in Srf activity is not a consequence of the relocalization of Srf protein through the activity of MuRF2.

We next asked whether Srf activity is modulated in muscle atrophy that has been triggered by different cues. Denervation-induced atrophy is due to sciatic nerve severing, leading to the

[1]Inserm U1016, Institut Cochin, F-75014 Paris, France. [2]CNRS UMR8104, F-75014 Paris, France. [3]Université Paris Descartes, F-75006 Paris, France.

*Author for correspondence (athanassia.sotiropoulos@inserm.fr)

Received 2 May 2014; Accepted 15 October 2014

Journal of Cell Science

Journal of Cell Science (2014) 127, 5157–5163 doi:10.1242/jcs.155911

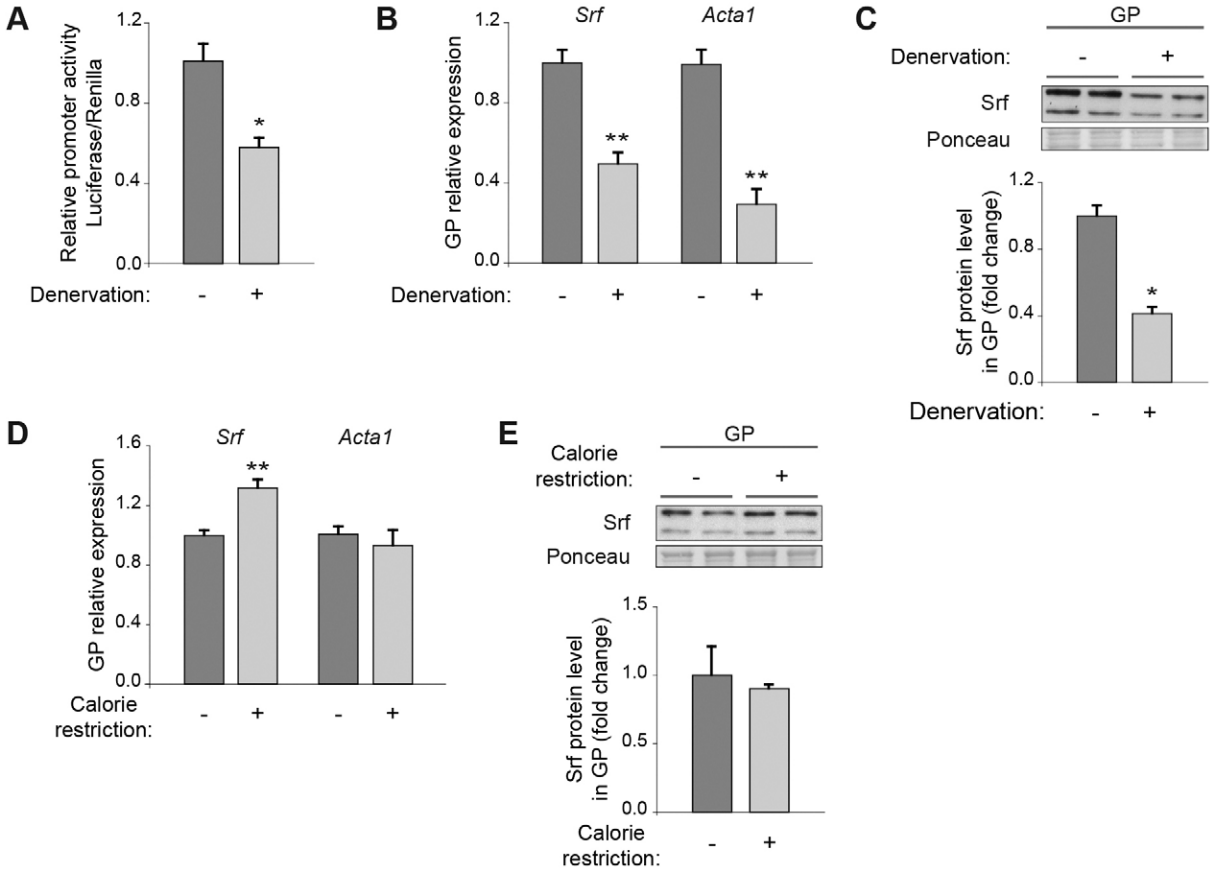

Fig. 1. Srf activity decreases upon disuse atrophy. (A) Responsiveness of an Srf reporter construct in tibialis anterior muscle from the contralateral leg or that of the denervated leg 7 days post denervation of control mice (n=3). (B) Normalized expression of *Srf* and *Acta1* in gastrocnemius and plantaris muscles from the contralateral leg or at 7 days post denervation (n=4). (C) Representative western blot analysis for Srf with Ponceau staining. Normalized fold change in Srf protein level in gastrocnemius and plantaris muscles (GP) 7 days post denervation (n=4). (D) Normalized expression of *Srf* and *Acta1* in the gastrocnemius and plantaris muscles of mice submitted to 7 days of calorie restriction or *ad libitum* feeding (n=4). (E) Representative western blot analyses for Srf with Ponceau staining. Normalized fold change in Srf protein level in gastrocnemius and plantaris muscles (GP) after 7 days of calorie restriction (n=3). Quantitative data are means±s.e.m. *P<0.05, **P<0.001.

suppression of nerve impulses, muscle contraction and stretching. Atrophy induced by gastrocnemius tenotomy entails the reduction of mechanical signals and the prevention of stretching whilst maintaining muscle innervation. In line with the results obtained upon denervation, the expression of *Acta1* and *Srf* was reduced in tenotomized gastrocnemius muscle (supplementary material Fig. S1D), suggesting that *in vivo* Srf activity is controlled through muscle stretching rather than through a trophic contribution of the nerve and excitation–contraction coupling.

Calorie-restriction-induced atrophy relies on nutrient shortage and not on the lack of mechanical cues. In contrast to observations following denervation and tenotomy, the expression of Srf targets was not downregulated after calorie restriction (Fig. 1D). *Srf* expression was even upregulated, but did not lead to increased Srf protein (Fig. 1E). Taken together, these data indicate that disuse, but not calorie-restriction-induced, muscle atrophy specifically leads to a sustained decrease in the overall activity of Srf.

Srf activity level regulates denervation-induced atrophy

To determine whether reduced Srf activity plays a functional role in denervation-induced atrophy, the extent of atrophy in denervated muscles from tamoxifen-injected HSA-Cre-ER^{T2}:Srf$^{flox/flox}$ mutant mice that lacked Srf in myofibers was analyzed (Fig. 2A; supplementary material Fig. S2A) (Guerci et al., 2012). After denervation, muscle weight and myofiber cross-sectional area (CSA) measurements revealed that mutant mice displayed a significantly higher atrophy of tibialis anterior, and gastrocnemius and plantaris muscles than those of control mice (Fig. 2B-D). This was not associated with higher expression levels of the ubiquitin ligases *MAFbx*, *MuRF1* and *Fbxo30* in mutant muscles, suggesting that their greater atrophy is not due to differences in the activation of the ubiquitin-proteasome pathway (supplementary material Fig. S2B). When subjected to calorie restriction, mutant and control mice presented similar extents of muscle atrophy (supplementary material Fig. S3), confirming the specific implication of Srf in disuse atrophy.

We then hypothesized that disuse atrophy could be counteracted by maintaining Srf activity through injection of control tibialis anterior muscles with adeno-associated viruses (AAVs) driving the expression of a constitutively active Srf derivative (AAV-SRFVP16) (Fig. 2E). Following denervation, overexpression of SRFVP16 induced a significant resistance to atrophy (Fig. 2F-H) and led to the persistence of endogenous *Srf* and *Acta1* transcript levels (supplementary material Fig. S2C). Collectively, these results demonstrate *in vivo* that the level of Srf activity modulates the extent of denervation-induced muscle atrophy. It is worth noting that, in non-denervated muscles, the

Journal of Cell Science (2014) 127, 5157–5163 doi:10.1242/jcs.155911

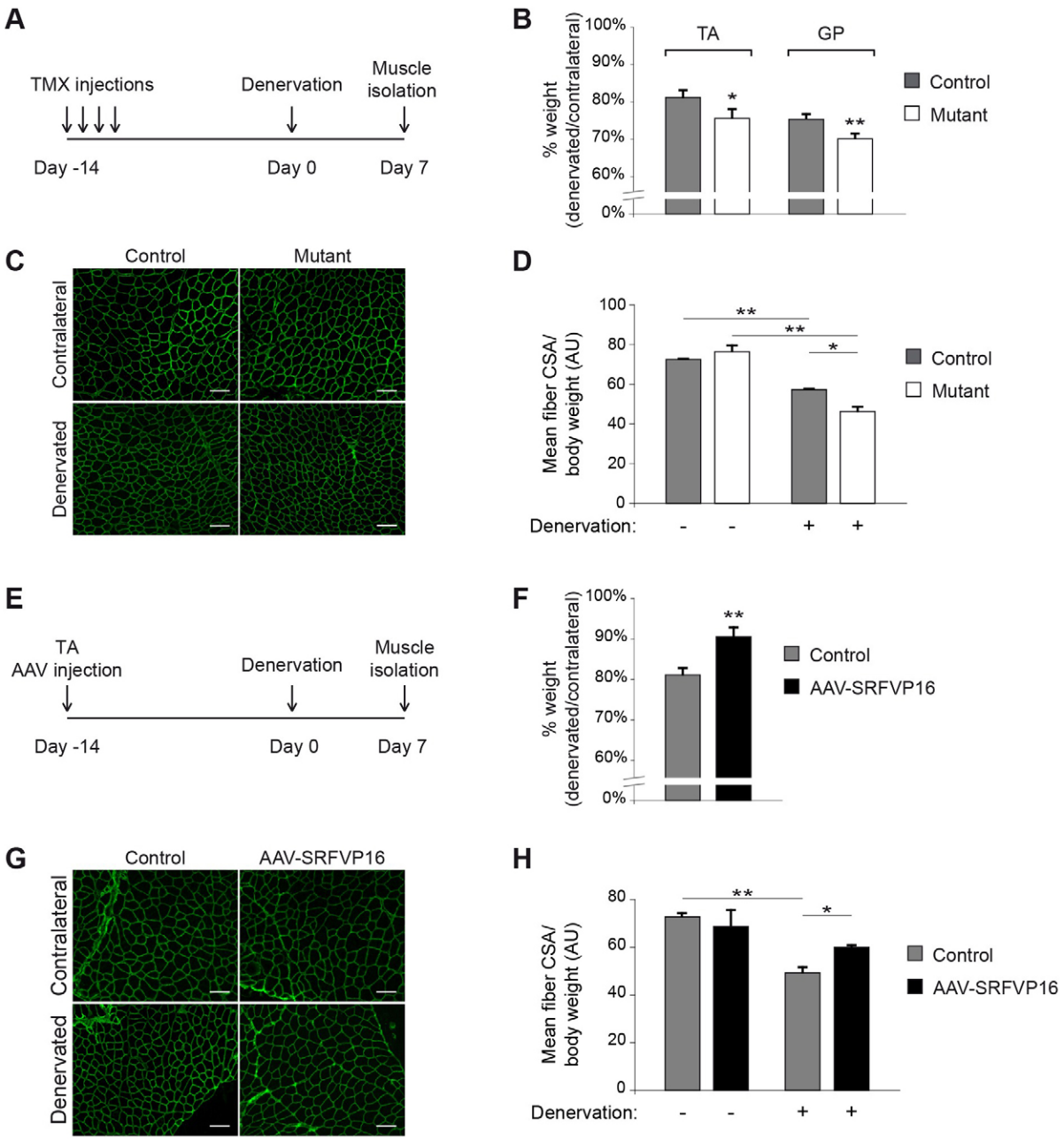

Fig. 2. The level of Srf activity regulates denervation-induced atrophy. (A) Control and Srf-mutant mice were injected with tamoxifen (TMX) 14 days before denervation. Muscles were isolated 7 days post denervation. (B) Ratio of the weight of the tibialis anterior (TA), and gastrocnemius and plantaris (GP) muscles 7 days post denervation to those of the contralateral leg of control and mutant mice (n=10). (C) Immunostaining of dystrophin in the contralateral and denervated leg tibialis anterior muscle of control and mutant mice 7 days post denervation. (D) Myofiber CSA to body weight ratio for tibialis anterior muscle in the denervated and contralateral legs in control and mutant mice 7 days post denervation (n=4). AU, arbitrary units. (E) Tibialis anterior muscles (TA) from control mice were injected (or not) with AAV-SRFVP16 14 days before denervation. Muscles were isolated 7 days post denervation. (F) Ratio of the weight of the tibialis anterior muscle 7 days post denervation to that of the contralateral leg of mice that had been injected (or not) with AAV-SRFVP16 (n=6). (G) Immunostaining of dystrophin in tibialis anterior muscle from the contralateral or denervated leg at 7 days post denervation that had been injected (or not) with AAV-SRFVP16. (H) Myofiber CSA to body weight ratio in tibialis anterior muscle from the contralateral or denervated leg at 7 days post denervation, which had been injected (or not) with AAV-SRFVP16 (n=4). Quantitative data are means±s.e.m. *P<0.05, **P<0.001. Scale bars: 100 μm.

activation or blunting of Srf activity does not change myofiber size (Fig. 2D,H), despite its effect on the expression of target genes such as *Acta1*. This suggests that, during denervation, a decrease in the activity of Srf leads to an amplification of the transcriptional atrophic program, acting in synergy with other pathways that are involved in protein catabolism.

Disuse leads to nuclear G-actin accumulation and subsequent exclusion of Mrtfs from myonuclei

We next asked which signaling pathway could result in a decrease of Srf activity upon disuse. Because biophysical stimuli can alter actin polymerization and because Srf activity can be regulated by actin dynamics, we hypothesized that disuse could lead to

Journal of Cell Science (2014) 127, 5157–5163 doi:10.1242/jcs.155911

alterations in monomeric G-actin quantity and/or localization. Strikingly, staining of G-actin, revealed by using fluorescent DNase I, showed that denervation induced a rapid and sustained accumulation of monomeric actin in myonuclei (Fig. 3A). By contrast, there was no difference in staining of G-actin between calorie-restricted and control muscles (Fig. 3A). Because Srf has been shown to control the expression of genes regulating actin treadmilling (Olson and Nordheim, 2010), the accumulation of nuclear G-actin could stem from a decrease of Srf activity upon disuse. Non-denervated *Srf*-deleted and AAV-SRFVP16-injected

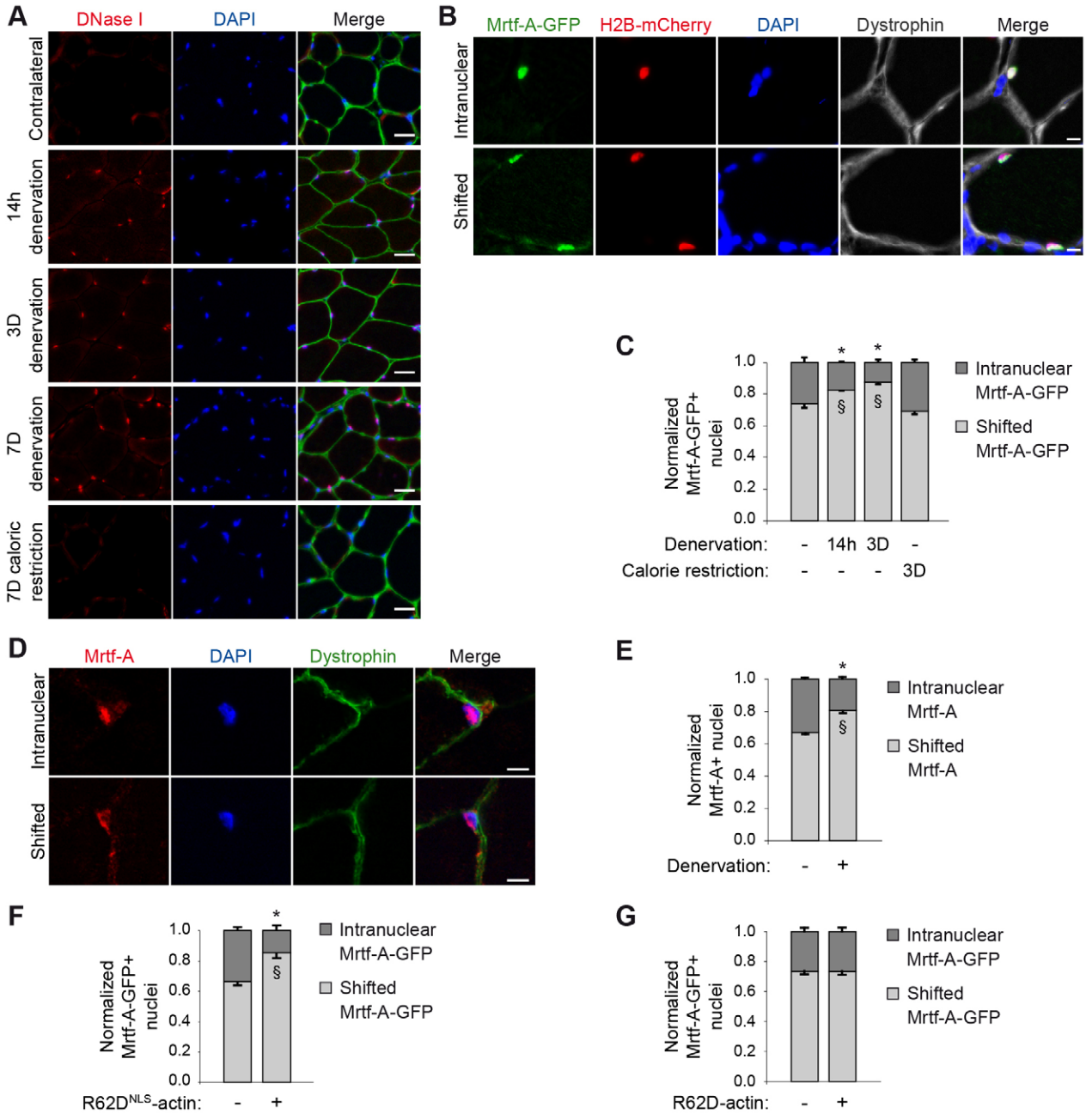

Fig. 3. Disuse leads to nuclear G-actin accumulation and subsequent exclusion of Mrtfs from myonuclei. (A) G-actin (DNase I), dystrophin (green) and DAPI staining in the tibialis anterior muscle of the contralateral leg, or that 14 h, 3 days (3D) or 7 days (7D) post denervation, or after 7 days of calorie restriction. (B) Intranuclear or shifted localization of overexpressed Mrtf-A–GFP in tibialis anterior muscle upon immunostaining of GFP. Nuclei are visualized through expression of H2B–mCherry and DAPI staining, and sarcolemma is identified through staining of dystrophin (gray). (C) Proportion of nuclei displaying intranuclear or shifted Mrtf-A–GFP localization in the tibialis anterior muscle of the contralateral leg, or at 14 h or 3 days (3D) post denervation, or after 3 days calorie restriction (n=3–4). (D) Intranuclear or shifted localization of endogenous Mrtf-A (red), dystrophin (green) and DAPI in tibialis anterior muscle. (E) Proportion of nuclei displaying intranuclear or shifted endogenous Mrtf-A localization in the contralateral or 3 days post denervation tibialis anterior muscle (n=4). (F) Proportion of nuclei displaying intranuclear or shifted Mrtf-A–GFP localization in tibialis anterior muscle that had been electroporated (or not) with R62D^{NLS}-actin (n=3). (G) Proportion of nuclei displaying intranuclear or shifted Mrtf-A–GFP localization in tibialis anterior muscle that had been electroporated (or not) with R62D-actin (n=3). Quantitative data are means±s.e.m. *P<0.05 vs intranuclear Mrtf-A–GFP (–), $^{§}P$<0.05 vs shifted Mrtf-A–GFP (–). Scale bars: 50 μm (A); 5 μm (B,D).

Journal of Cell Science (2014) 127, 5157–5163 doi:10.1242/jcs.155911

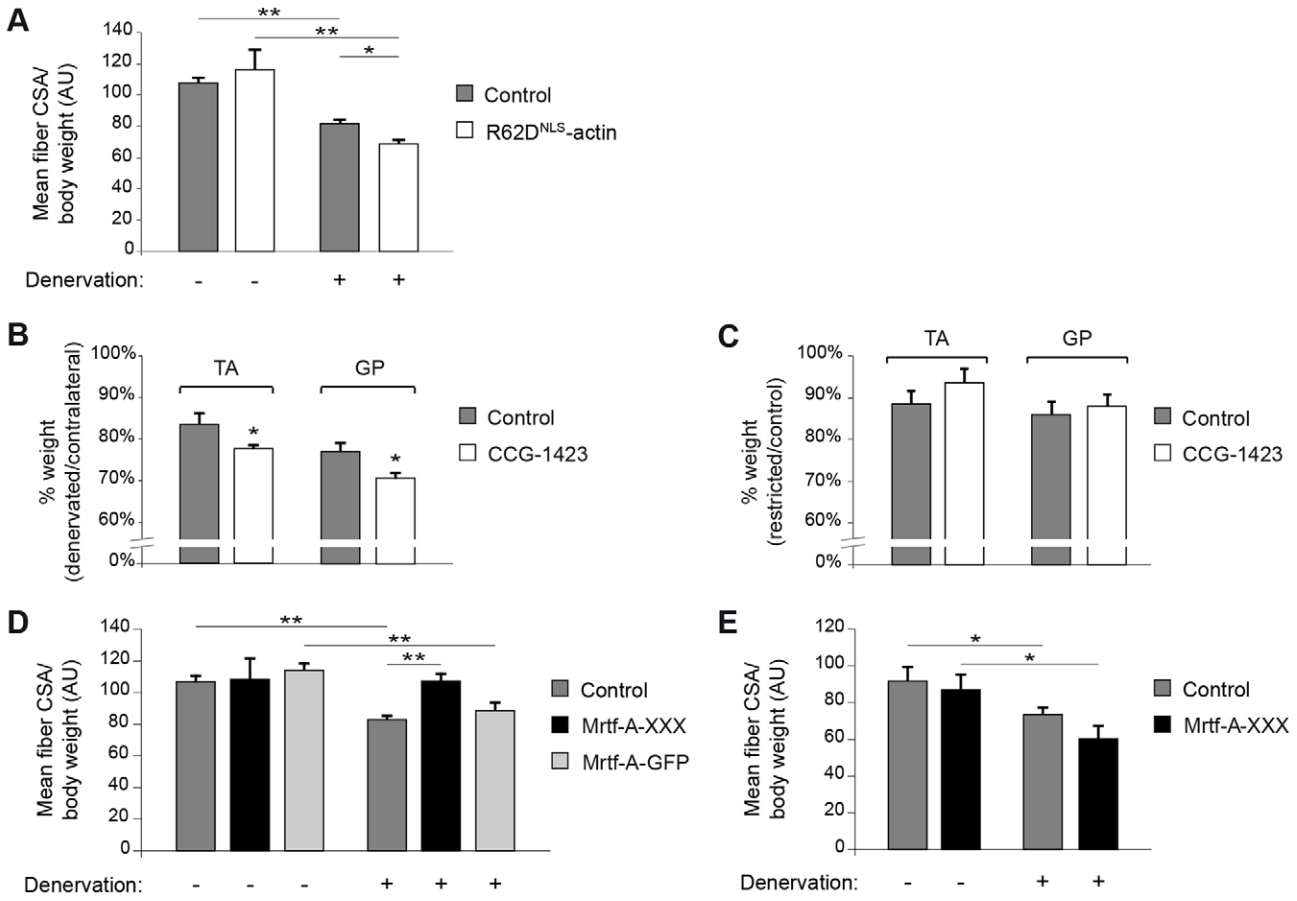

Fig. 4. The actin–Mrtfs–Srf pathway controls disuse atrophy. (A) Myofiber CSA to body weight ratio for tibialis anterior muscle from the contralateral leg or that 7 days post denervation, electroporated (or not) with R62D^{NLS}-actin (n=3–17). (B) Ratio of the weight of the tibialis anterior (TA), and gastrocnemius and plantaris (GP) muscles 7 days post denervation to those of the contralateral leg of control mice that had been injected with CCG-1423 or vehicle, (n=5). (C) Ratio of the weight of the tibialis anterior (TA), and gastrocnemius and plantaris (GP) muscles after 7 days of calorie restriction to those of control mice that had been injected with CCG-1423 or vehicle (n=5). (D) Myofiber CSA to body weight ratio for tibialis anterior muscle 7 days post denervation or from the contralateral leg, electroporated (or not) with Mrtf-A-XXX or Mrtf-A–GFP (n=4–17). (E) The ratio of the S*rf*-deleted myofiber CSA to body weight for tibialis anterior muscle 7 days post denervation or from the contralateral leg, electroporated (or not) with Mrtf-A-XXX (n=3–4). Quantitative data are means±s.e.m. *P<0.05, **P<0.001. AU, arbitrary units.

muscles showed the same G-actin staining as that in control muscles (supplementary material Fig. S4A), indicating that nuclear G-actin accumulation following denervation is a consequence of disuse and not of a reduction in Srf activity. Moreover, our data establish a link between the increase in nuclear G-actin levels and a physiopathologically relevant condition, muscle disuse atrophy.

Actin dynamics control Srf activity by regulating the subcellular localization of Mrtfs – G-actin binds to Mrtfs, inhibiting their entry into (Pawlowski et al., 2010) and stimulating their export from nuclei (Vartiainen et al., 2007). To determine whether the increased levels of nuclear G-actin caused by denervation are correlated with the altered subcellular localization of Mrtfs, tibialis anterior muscles were electroporated with a plasmid encoding Mrtf-A tagged with green fluorescent protein (Mrtf-A–GFP), together with a Histone2B-mCherry plasmid to identify electroporated myofiber nuclei. Immunostaining for GFP revealed two different subcellular localizations of Mrtf-A – intranuclear, characterized by an exact colocalization of Mrtf-A–GFP with mCherry-tagged Histone 2B (H2B–mCherry), and shifted, in which some Mrtf-A–GFP did not colocalize with chromatin (Fig. 3B; supplementary material S4B,C and illustrated by 3D reconstructions in supplementary material Fig. S4D). In addition, immunostaining for Emerin suggested that at least some Mrtf-A–GFP is perinuclear and located outside of the nuclear envelope (supplementary material Fig. S4E,F). Importantly, denervation led to a rapid decrease in intranuclear Mrtf-A–GFP (Fig. 3C). In line with this, immunostaining for endogenous Mrtf-A confirmed that denervation diminished Mrtf-A localization in myonuclei (Fig. 3D,E). By contrast, there was no difference in the distribution of Mrtf-A–GFP in muscle from mice that had been fed in a normal or restricted manner (Fig. 3C). Taken together, these data show that Mrtf-A nuclear exclusion is a specific response to changes in mechanical load.

As post-denervation kinetics of nuclear G-actin accumulation coincide with that of decreasing intranuclear Mrtf-A, we speculated that an increase in nuclear G-actin could induce Mrtf-A shuttling out of myonuclei. To test this hypothesis, we artificially elevated the amount of nuclear G-actin by electroporating tibialis anterior muscle with a R62D^{NLS}-actin plasmid, which encodes a constitutively nuclear non-polymerizable actin derivative (supplementary material Fig. S4G), together with the Mrtf-A–GFP plasmid. Overexpression of R62D^{NLS}-actin in non-denervated muscle was sufficient to exclude Mrtf-A–GFP from myonuclei to a

similar extent to that observed post denervation (Fig. 3F). In fibroblasts, it has been shown that the interaction between G-actin and Mrtfs can occur in both the nucleus and cytoplasm (Vartiainen et al., 2007). Interestingly, overexpression of R62D-actin, leading to an accumulation of G-actin predominantly in the cytoplasm (supplementary material Fig. S4H), did not change Mrtf-A–GFP localization, suggesting that, in muscle tissue, shuttling of Mrtfs, and subsequent activation of Srf–Mrtf, is principally modulated by nuclear G-actin and does not involve the regulation of cytosolic actin pathways (Fig. 3G). As G-actin shuttles actively between cytoplasm and nuclei through specific transporters, G-actin transport could be affected by loss of mechanical cues, resulting in its nuclear accumulation. Furthermore, actin polymerization and depolymerization processes also take place in nuclei and could modulate nuclear G-actin content (Grosse and Vartiainen, 2013). In particular, the nuclear actin regulatory protein Mical-2 has been shown to lower the amount of nuclear G-actin (Lundquist et al., 2014), and denervated muscles exhibited a reduction of *Mical-2* expression (supplementary material Fig. S4I). We can thus speculate that abolition of mechanical signals increases nuclear G-actin by disrupting nuclear actin dynamics through the deregulation of actin regulatory proteins, such as Mical-2.

The actin–Mrtf–Srf pathway controls disuse atrophy

We next sought to ascertain the role of the actin–Mrtf–Srf pathway in regulating disuse atrophy. Because denervation-induced atrophy is aggravated in muscles that lack Srf, we hypothesized that atrophy should also be worsened through reducing the activity of Srf–Mrtf by using $R62D^{NLS}$-actin. In line with the increased Mrtf-A–GFP nuclear exclusion that is induced through $R62D^{NLS}$-actin (Fig. 3F), $R62D^{NLS}$-actin-electroporated tibialis anterior muscle showed a higher denervation-induced atrophy than control muscles, mimicking the *Srf*-knockout phenotype (Fig. 4A). Mrtfs-dependent Srf activity can also be inhibited by using the compound CCG-1423 (Minami et al., 2012). Tibialis anterior, and gastrocnemius and plantaris muscles of CCG-1423-injected mice were more atrophied after denervation than the muscles of vehicle-injected mice, whereas calorie-restriction-induced atrophy was unaffected (Fig. 4B,C). These data show *in vivo* that specific downregulation of the activity of Mrtfs aggravates disuse muscle atrophy.

To determine whether muscle atrophy could be rescued by maintaining high activity levels of Mrtfs, we overexpressed in myofibers a constitutively active Mrtf-A derivative (Mrtf-A-XXX), which is defective for actin binding and is located inside myonuclei exclusively (supplementary material Fig. S4J). Fibers that expressed Mrtf-A-XXX became completely resistant to denervation-induced atrophy (Fig. 4D), suggesting that, among Srf cofactors, Mrtfs are the main modulators of Srf activity in this system. Interestingly, Mrtf-A–GFP, which has wild-type actin-binding sites, did not rescue atrophy (Fig. 4D), strongly supporting a crucial role for the binding of G-actin to Mrtfs in the muscle atrophic response to disuse.

Mrtfs have been shown to interact with other transcription regulators, such as Smads (Charbonney et al., 2011; Wang et al., 2012). In order to investigate whether the atrophy resistance induced by active Mrtf-A requires Srf, Mrtf-A-XXX was electroporated into muscles that lacked Srf. Denervated mutant muscles displayed the same level of atrophy, regardless of Mrtf-A-XXX overexpression (Fig. 4E), demonstrating that the resistance to denervation-induced atrophy conferred by Mrtf-A-XXX depends on Srf.

In conclusion, our study shows that the alteration of any components of the actin–Mrtf–Srf pathway is sufficient to affect the extent of disuse muscle atrophy and identifies nuclear G-actin and Mrtfs as the main upstream regulators that are involved. Our data provide novel genetic and mechanistic insights into how muscle mass is regulated through a lack of mechanical stimulation and unravels the actin–Mrtf–Srf axis as a key specific regulator of disuse atrophy, establishing a link with human pathophysiological atrophy due to inactivity, nerve injury or motor neuron diseases. Therapeutic targeting of the actin–Mrtf–Srf pathway might improve the condition and quality of life of an individual with disuse muscle atrophy because maintaining the activity of Mrtfs fully counteracts the phenotype.

MATERIALS AND METHODS

Mouse protocols

$Srf^{flox/flox}$ and HSA-Cre-ER^{T2}:$Srf^{flox/flox}$ mice have been described previously (Lahoute et al., 2008). Two-month-old HSA-Cre-ER^{T2}:$Srf^{flox/flox}$ and $Srf^{flox/flox}$ males were given four tamoxifen injections (1 mg/day; Sigma) and are referred as mutant and control mice, respectively.

Denervation was performed by sectioning the sciatic nerve of one leg. The intact contralateral leg was used as an internal control. For calorie restriction, mice were placed in individual cages and fed with 50% of the daily food amount or fed *ad libitum*. Where indicated, mice were injected intraperitoneally and daily with CCG-1423 (0.15 mg/kg; Cayman Chemical) or vehicle. Treatment with CCG-1423 started 2 days prior to and then during the timeframe of the experiment.

Gene electrotransfer was performed as described previously (Guerci et al., 2012). Tibialis anterior muscles were injected with the indicated plasmids: 1 µg Mrtf-A–GFP+3 µg H2B–mCherry+5 µg empty vector; 10 µg Mrtf-A-XXX or R62D-actin or $R62D^{NLS}$-actin+3 µg H2B–mCherry; 5 µg 3DA-luciferase+2 µg TK-*Renilla*+5 µg empty vector. Mice were denervated or calorie restricted 7 days after electroporation. Reporter assays were performed using the Dual-Luciferase kit (Promega).

AAV-SRFVP16 particles were produced as described previously (Guerci et al., 2012). AAV transduction was performed by injecting tibialis anterior muscles with 1.87×10^{10} viral genomes 14 days before denervation.

All experiments were conducted in accordance with the European guidelines for the care and use of laboratory animals and were approved by the institutional ethic committee (number 00315.01).

Plasmids

The Srf-reporter construct (3DA-luciferase: 3 CArGs upstream *Luciferase* gene) has been described previously (Geneste et al., 2002). The TK-*Renilla* plasmid (Promega) was used as an electroporation efficiency control. Plasmid H2B–mCherry encodes the Histone-2B–mCherry fusion protein (Abgene). Plasmids encoding hemagglutinin (HA)-tagged-Mrtf-A-XXX, Mrtf-A–GFP, HA-tagged-R62D-actin and Flag-tagged-$R62D^{NLS}$-actin have been described previously (Guettler et al., 2008; Posern et al., 2002; Stern et al., 2009; Vartiainen et al., 2007).

RNA extraction and qRT-PCR

RNA extraction and quantitative real-time (qRT)-PCR analysis were performed as described previously (Guerci et al., 2012). Values were normalized using *Hydroxymethylbilane synthase* (*Hmbs*). The following primers were used: *Acta1*-F, 5′-CTGAGCGCAAGTACTCAGTGTGGA-3′; *Acta1*-R, 5′-TTCCAAAAACAGGCGCCGGCTGCA-3′; *Srf*-F, 5′-CACCTACCAGGTGTCGGAAT-3′; *Srf*-R, 5′-GCTGTGTGGATTGT-GGAGGT-3′; *Hmbs*-F, 5′-TGCACGATCCTGAAACTCTG-3′; *Hmbs*-R, 5′-TGCATGCTATCTGAGCCATC-3′.

Immunostaining

Muscle cryosections (8 µm) were fixed in 4% paraformaldehyde for 8 min, blocked in 5% goat serum, 4% BSA, 0.2% Triton

X-100 in PBS, incubated overnight with primary antibodies, washed with PBS, incubated with appropriate secondary antibodies and counterstained with DAPI. Tibialis anterior muscles overexpressing Mrtf-A–GFP were prefixed in 4% paraformaldehyde for 2 h and incubated overnight in 40% sucrose before freezing. The primary antibodies used were against Srf and Mrtf-A (Santa Cruz), dystrophin (Novocastra), laminin-α2 and GFP (Abcam), HA (Roche), Flag (Sigma) and emerin (Novus Biologicals). For G-actin staining, Texas-Red-conjugated DNase-I was used following the manufacturer's protocol (Molecular Probes).

Image acquisition

Digital images were acquired using a Zeiss Axiovert 200M microscope with 10×, 20× or 40× magnification, or using a Spinning Disk Leica confocal microscope with a 100× oil-immersion objective, cooled CCD CoolSNAP-HQ^2 camera (Photometrics) and Metamorph 7.7.5 (Molecular Devices). Images were composed and edited in Adobe Photoshop and ImageJ. Background was reduced using brightness and contrast adjustments applied to the whole image. Three-dimensional reconstitutions from confocal microscopy images were performed using Imaris 7.2 (Bitplane).

Morphometric analyses

Myofiber CSA was analyzed by using immunostaining of dystrophin, marking myofiber sarcolemma, and then using Metamorph. Between 1000 and 1500 myofibers were analyzed per non-electroporated or AAV-injected muscle. For electroporated tibialis anterior muscle, 40–200 myofibers (positive for HA-Mrtf-A-XXX, Flag-R62D^{NLS}-actin or Mrtf-A–GFP) were analyzed.

Quantification of Mrtf-A–GFP subcellular distribution was performed on Mrtf-A–GFP-positive and H2B–mCherry-positive myonuclei (30–250 myonuclei/muscle). For endogenous Mrtf-A, 40–120 myonuclei/muscle were analyzed.

Western blotting analysis

Western blotting was performed as described previously (Lahoute et al., 2008). Immunoblots were hybridized with anti-Srf antibody and normalized by using Ponceau staining. Protein bands were quantified by using Bio-Rad Quantity One (version 4.6.6).

Statistical analysis

Statistics were performed by using SigmaPlot 12.5 (Systat). When two groups were compared, the significance of differences between the means was assessed with a Student's *t*-test after normality and equal variance tests were passed. For multiple comparison, a two-way ANOVA test was used after normality and equal variance tests were passed and was followed by using a Bonferroni *t*-test for pairwise multiple comparison. *P*-values of <0.05 were considered statistically significant.

Acknowledgements

We thank Richard Treisman (Cancer Research UK, London, UK) and Guido Posern (Institute for Physiological Chemistry, Halle, Germany) for providing materials. We are grateful to Pascal Maire (Cochin Institute, Paris, France), Luisa Dandolo (Cochin Institute, Paris, France), Anne Lombès (Cochin Institute, Paris, France) and Dominique Daegelen (Cochin Institute, Paris, France) for critical reading of the manuscript.

Competing interests

The authors declare no competing interests.

Author contributions

L.C. designed and carried out experiments, analyzed results and wrote the manuscript. G.H. and A.P. conducted experiments and analyzed results. V.R-H. and A.G. provided expertise in physiological analysis. A.S. designed and carried out experiments, analyzed results, wrote the manuscript and provided financial support.

Funding

This work was supported by The French Muscular Dystrophy Association (AFM); Agence Nationale de la Recherche (ANR) [grant JC08-327703; 13-BSV1-0005-01]; and Labex WhoAmI.

Supplementary material

Supplementary material available online at
http://jcs.biologists.org/lookup/suppl/doi:10.1242/jcs.155911/-/DC1

References

Bonaldo, P. and Sandri, M. (2013). Cellular and molecular mechanisms of muscle atrophy. *Dis. Model. Mech.* **6**, 25-39.

Charbonney, E., Speight, P., Masszi, A., Nakano, H. and Kapus, A. (2011). β-catenin and Smad3 regulate the activity and stability of myocardin-related transcription factor during epithelial-myofibroblast transition. *Mol. Biol. Cell* **22**, 4472-4485.

Geneste, O., Copeland, J. W. and Treisman, R. (2002). LIM kinase and Diaphanous cooperate to regulate serum response factor and actin dynamics. *J. Cell Biol.* **157**, 831-838.

Giger, J. M., Bodell, P. W., Zeng, M., Baldwin, K. M. and Haddad, F. (2009). Rapid muscle atrophy response to unloading: pretranslational processes involving MHC and actin. *J. Appl. Physiol.* **107**, 1204-1212.

Grosse, R. and Vartiainen, M. K. (2013). To be or not to be assembled: progressing into nuclear actin filaments. *Nat. Rev. Mol. Cell Biol.* **14**, 693-697.

Guerci, A., Lahoute, C., Hébrard, S., Collard, L., Graindorge, D., Favier, M., Cagnard, N., Batonnet-Pichon, S., Précigout, G., Garcia, L. et al. (2012). Srf-dependent paracrine signals produced by myofibers control satellite cell-mediated skeletal muscle hypertrophy. *Cell Metab.* **15**, 25-37.

Guettler, S., Vartiainen, M. K., Miralles, F., Larijani, B. and Treisman, R. (2008). RPEL motifs link the serum response factor cofactor MAL but not myocardin to Rho signaling via actin binding. *Mol. Cell. Biol.* **28**, 732-742.

Lahoute, C., Sotiropoulos, A., Favier, M., Guillet-Deniau, I., Charvet, C., Ferry, A., Butler-Browne, G., Metzger, D., Tuil, D. and Daegelen, D. (2008). Premature aging in skeletal muscle lacking serum response factor. *PLoS ONE* **3**, e3910.

Lange, S., Xiang, F., Yakovenko, A., Vihola, A., Hackman, P., Rostkova, E., Kristensen, J., Brandmeier, B., Franzen, G., Hedberg, B. et al. (2005). The kinase domain of titin controls muscle gene expression and protein turnover. *Science* **308**, 1599-1603.

Lundquist, M. R., Storaska, A. J., Liu, T. C., Larsen, S. D., Evans, T., Neubig, R. R. and Jaffrey, S. R. (2014). Redox modification of nuclear actin by MICAL-2 regulates SRF signaling. *Cell* **156**, 563-576.

Minami, T., Kuwahara, K., Nakagawa, Y., Takaoka, M., Kinoshita, H., Nakao, K., Kuwabara, Y., Yamada, Y., Yamada, C., Shibata, J. et al. (2012). Reciprocal expression of MRTF-A and myocardin is crucial for pathological vascular remodelling in mice. *EMBO J.* **31**, 4428-4440.

Ochala, J., Gustafson, A. M., Diez, M. L., Renaud, G., Li, M., Aare, S., Qaisar, R., Banduseela, V. C., Hedström, Y., Tang, X. et al. (2011). Preferential skeletal muscle myosin loss in response to mechanical silencing in a novel rat intensive care unit model: underlying mechanisms. *J. Physiol.* **589**, 2007-2026.

Olson, E. N. and Nordheim, A. (2010). Linking actin dynamics and gene transcription to drive cellular motile functions. *Nat. Rev. Mol. Cell Biol.* **11**, 353-365.

Pawłowski, R., Rajakylä, E. K., Vartiainen, M. K. and Treisman, R. (2010). An actin-regulated importin α/β-dependent extended bipartite NLS directs nuclear import of MRTF-A. *EMBO J.* **29**, 3448-3458.

Pipes, G. C., Creemers, E. E. and Olson, E. N. (2006). The myocardin family of transcriptional coactivators: versatile regulators of cell growth, migration, and myogenesis. *Genes Dev.* **20**, 1545-1556.

Polge, C., Heng, A. E., Jarzaguet, M., Ventadour, S., Claustre, A., Combaret, L., Béchet, D., Matondo, M., Uttenweiler-Joseph, S., Monsarrat, B. et al. (2011). Muscle actin is polyubiquitinylated in vitro and in vivo and targeted for breakdown by the E3 ligase MuRF1. *FASEB J.* **25**, 3790-3802.

Posern, G. and Treisman, R. (2006). Actin' together: serum response factor, its cofactors and the link to signal transduction. *Trends Cell Biol.* **16**, 588-596.

Posern, G., Sotiropoulos, A. and Treisman, R. (2002). Mutant actins demonstrate a role for unpolymerized actin in control of transcription by serum response factor. *Mol. Biol. Cell* **13**, 4167-4178.

Stern, S., Debre, E., Stritt, C., Berger, J., Posern, G. and Knöll, B. (2009). A nuclear actin function regulates neuronal motility by serum response factor-dependent gene transcription. *J. Neurosci.* **29**, 4512-4518.

Vartiainen, M. K., Guettler, S., Larijani, B. and Treisman, R. (2007). Nuclear actin regulates dynamic subcellular localization and activity of the SRF cofactor MAL. *Science* **316**, 1749-1752.

Wang, D., Prakash, J., Nguyen, P., Davis-Dusenbery, B. N., Hill, N. S., Layne, M. D., Hata, A. and Lagna, G. (2012). Bone morphogenetic protein signaling in vascular disease: anti-inflammatory action through myocardin-related transcription factor A. *J. Biol. Chem.* **287**, 28067-28077.